Asymmetric Pareto-adaptive Scheme for Multiobjective Optimization

Siwei Jiang, Jie Zhang, Yew Soon Ong

School of Computer Engineering, Nanyang Technology University, Singapore
{sjiang1,zhangj,asysong}@ntu.edu.sg

Abstract. A core challenge of Multiobjective Evolutionary Algorithms (MOEAs) is to attain evenly distributed Pareto optimal solutions along the Pareto front. In this paper, we propose a novel asymmetric Pareto-adaptive (apa) scheme for the identification of well distributed Pareto optimal solutions based on the geometrical characteristics of the Pareto front. The apa scheme applies to problem with symmetric and asymmetric Pareto fronts. Evaluation on multiobjective problems with Pareto fronts of different forms confirms that apa improves both convergence and diversity of the classical decomposition-based (MOEA/D) and Pareto dominance-based MOEAs ($pa\epsilon$-MyDE).

Keywords: Multiobjective Optimization, Hypervolume, Pareto-adaptive

1 Introduction

Multiobjective optimization problems (MOPs) involve several conflicting objectives to be optimized simultaneously. For Pareto optimal solutions, improvement on one objective leads to the decrement of at least one other objective. Multiobjective Evolutionary Algorithms (MOEAs) have been well established as efficient approaches to deal with various MOPs [1].

MOEAs can be generally categorized into two major classes, namely decomposition-based (MOEA/D) and Pareto dominance-based MOEAs [2]. MOEA/D decomposes MOPs into a number of scalar subproblems and optimizes them simultaneously. The assigned weight vectors of classical MOEA/D, however, may not always suit different *Pareto front* (PF). Pareto dominance-based MOEAs use the Pareto dominance definition with the crowding distance or neighbor density estimator to evaluate individuals. However, both of them are less effective to deal with MOPs with asymmetric PFs.

In this paper, we propose a novel asymmetric Pareto-adaptive (apa) scheme. Driven by the hypervolume [3–5] , apa is designed to evenly distribute Pareto optimal solutions along both asymmetric and symmetric PFs. Experimental results on different shapes of 2-dimensional MOPs showed that MOEA/D and $pa\epsilon$-MyDE (one from each category of MOEAs) using apa, labeled here as $apa\lambda$-MOEA/D and $apa\epsilon$-MyDE respectively, lead to higher hypervolume, better convergence and more evenly distributed solutions.

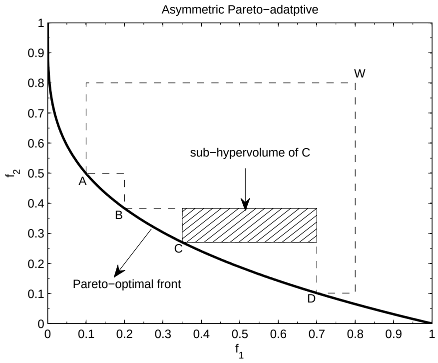

Fig. 1. Asymmetric Pareto-adaptive Scheme

2 *apa*: Asymmetric Pareto-adaptive

2.1 *apa* for 2-Dimensional Pareto Front

The new asymmetric Pareto-adaptive (apa) scheme is driven by the hypervolume. When minimizing bi-objectives for instance, hypervolume is the area enclosed within the discontinuous dash line *WABCDW* (Figure 1). $X = \{A, B, C, D\}$ denotes the set of non-dominated solutions and W is the reference point constructed by the worst objective function values.

Assume points $\{A, B, D\}$ are fixed and point C moves along curve BD. The hypervolume of X is then decided by the sub-hypervolume of point C, which is indicated by the shaded rectangle. In general, we define the normalized asymmetric Pareto optimal front as $f_1^{p_1} + f_2^{p_2} = 1$, where $p_1 \neq p_2$. The points on the curve are $B(x_1, y_1), C(x, y)$, $D(x_2, y_2)$, and the sub-hypervolume of point C is calculated as:

$$\vartheta(x) = (x_2 - x)(y_1 - y) = xy - y_1 x - x_2 y + x_2 y_1 \tag{1}$$

To maximize sub-hypervolume, the optimal position of point C is $(\hat{x}, \hat{y} = (1 - \hat{x}^{p_1})^{\frac{1}{p_2}})$, which can be calculated by the Newton Iterative method defined as:

$$x_{k+1} = x_k - \vartheta'(x_k)/\vartheta''(x_k) \tag{2}$$

where $\vartheta'(x)$ and $\vartheta''(x)$ are the first and second order of $\vartheta(x)$, respectively. The initial value $x_0 = (x_1 + x_2)/2$. When stopping criteria $x_{k+1} - x_k < \xi$ is satisfied, $\hat{x} = x_{k+1}$. The maximum sub-hypervolume is calculated as $\vartheta(\hat{x})$.

Algorithm 1 presents the details of the apa scheme. The N initial points $X = \{(x_1, y_1), \cdots, (x_N, y_N)\}$ along PF are constructed by equally dividing the f_1 axis (Line 1). In Line 9, the point (x_{i_m}, y_{i_m}) is replaced by $(\hat{x}_{i_m}, \hat{y}_{i_m})$, which makes the maximum increment to the hypervolume. In Lines 10-14, the movement of point i_m only impact the neighborhood points. We update the sub-hypervolume and the maximum sub-hypervolume of the neighborhood points $(i_m - 1, i_m, i_m + 1)$. When the hypervolume increment is less than ξ, the algorithm terminates and outputs X.

Algorithm 1: Asymmetric Pareto-adaptive scheme

Initialize N points X along Pareto optimal front
Sort the N points ascending by the first objective
for $i = 2, \cdots, N-1$ **do**
  Calculate sub-hypervolume $\vartheta(x_i)$
  Calculate maximum sub-hypervolume $\vartheta(\hat{x}_i)$
  $\triangle\vartheta(x_i) = \vartheta(x_i) - \vartheta(\hat{x}_i)$
Find $i_m = \max\{\triangle\vartheta(x_i) : i \in 2, \cdots, N-1\}$
while $\triangle\vartheta(x_{i_m}) > \xi$ **do**
  Move the point (x_{i_m}, y_{i_m}) to $(\hat{x}_{i_m}, \hat{y}_{i_m})$
  Set $\vartheta(x_{i_m}) = \vartheta(\hat{x}_{i_m})$, $\triangle\vartheta(x_{i_m}) = 0$
  Update $\vartheta(x_{i_m-1})$ and $\vartheta(x_{i_m+1})$
  Update $\vartheta(\hat{x}_{i_m-1})$ and $\vartheta(\hat{x}_{i_m+1})$
  $\triangle\vartheta(x_{i_m-1}) = \vartheta(x_{i_m-1}) - \vartheta(\hat{x}_{i_m-1})$
  $\triangle\vartheta(x_{i_m+1}) = \vartheta(x_{i_m+1}) - \vartheta(\hat{x}_{i_m-1})$
  Find $i_m = \max\{\triangle\vartheta(x_i) : i \in 2, \cdots, N-1\}$
Output X

2.2 Curve Function for Asymmetric Pareto Front

Upon generating a set of Pareto optimal solutions (points), we estimate a curve function to represent the PF based on the available points. Define 2D Pareto optimal solutions as $F = \{(x_i, y_i) : i = 1, \cdots, |F|\}$ ($|F|$ is the number of points, normalized into $[0, 1]$). To estimate the asymmetric PF $f_1^{p_1} + f_2^{p_2} = 1$, we define the Sum of Square Error as:

$$SSE(F) = \sum_i^{|F|} (x_i^{p_1} + y_i^{p_2} - 1 + \theta)^2 \quad (3)$$

where θ denotes the relaxing parameter. A small $SSE(F)$ implies that the curve function approaches the Pareto optimal solutions better. In reality, it is not easy for all solutions to fall exactly on the true PF, thus, it is natural to set the relaxing parameter with a small value to estimate the curve function.

3 apa for Decomposition and ϵ-dominance

The well established two major categories of MOEAs includes the decomposition-based and Pareto dominance-based MOEAs. In this section, we describe how the apa scheme enhances the performances of MOEAs.

3.1 $apa\lambda$: apa for Decomposition

MOEA based on decomposition (MOEA/D) transforms the PF into a number of scalar optimization subproblems and optimizes them simultaneously. Three major approaches of the MOEA/D are weighted sum, Tchebycheff and Boundary intersection (BI) [2].

Define $\lambda = (\lambda^1, \cdots, \lambda^m)^T$ as a weight vector for m objectives, and $\sum_i^m \lambda^i = 1$. Classical MOEA/D produces N weight vectors in 2-dimensional objective spaces as: $(\frac{0}{H}, \frac{H}{H}), (\frac{1}{H}, \frac{H-1}{H}), \cdots, (\frac{H}{H}, \frac{0}{H})$, where $H = N - 1$. The gradients of weight vectors are represented by λ lines (see Figures 2, 3). These λ lines produce N intersection points along PF. Such weight vectors are perfectly distributed only when PF is $f_1 + f_2 = 1$ (i.e. a linear line), but not suitable for $f_1^{p_1} + f_2^{p_2} = 1, p_1, p_2 \neq 1$ (i.e. non-linear PF).

Asymmetric Pareto-adaptive weight vectors ($apa\lambda$) is formed by applying the apa scheme to MOEA/D. Since the apa scheme (Algorithm 1) can obtain evenly distributed intersection points $\{(x_i, y_i), i = 1, \cdots, N\}$ along different shapes of Pareto optimal front, the weight vectors along asymmetric Pareto optimal front can be adjusted as:

$$apa\lambda_i = (\frac{x_i}{x_i + y_i}, \frac{y_i}{x_i + y_i}) \tag{4}$$

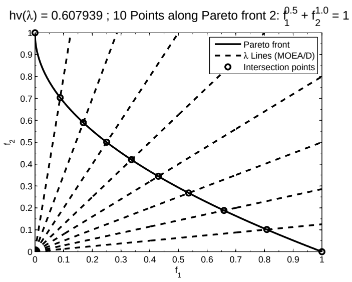

(a) λ for asymmetric convex PF

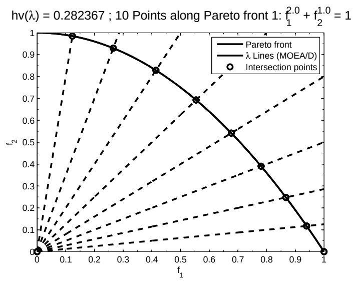

(b) λ for asymmetric concave PF

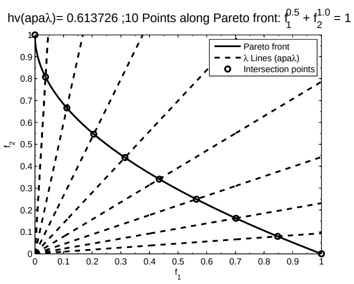

(c) $apa\lambda$ for asymmetric convex PF

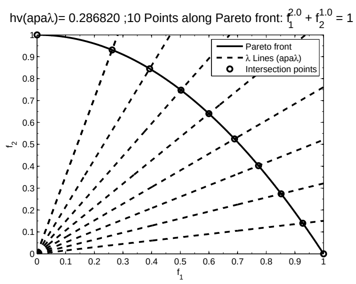

(d) $apa\lambda$ for asymmetric concave PF

Fig. 2. 10 Points along 2-dimensional *asymmetric* Pareto Fronts by λ and $apa\lambda$

Figure 2 shows an example of 10 intersection points along 2-dimensional asymmetric PFs generated by λ (MOEA/D) and the $apa\lambda$ scheme, respectively. When p_1=0.5, p_2=1.0, the hypervolume of the intersection points is $hv(\lambda) = 0.607939$ in MOEA/D (Figure 2(a)). From Figure 2(c), $apa\lambda$ obtains a larger $hv(apa\lambda) = 0.613726$, and the λ lines are scattered to the two endpoints of PF and distributed more evenly. When $p_1 = 2.0$ and $p_2 = 1.0$, the hypervolume of intersection points is $hv(\lambda) = 0.282367$ in MOEA/D (Figure 2(b)). $apa\lambda$ obtains a larger $hv(apa\lambda) = 0.286820$ (Figure 2(d)), and the λ lines are well assembled and divide the objective space more uniformly.

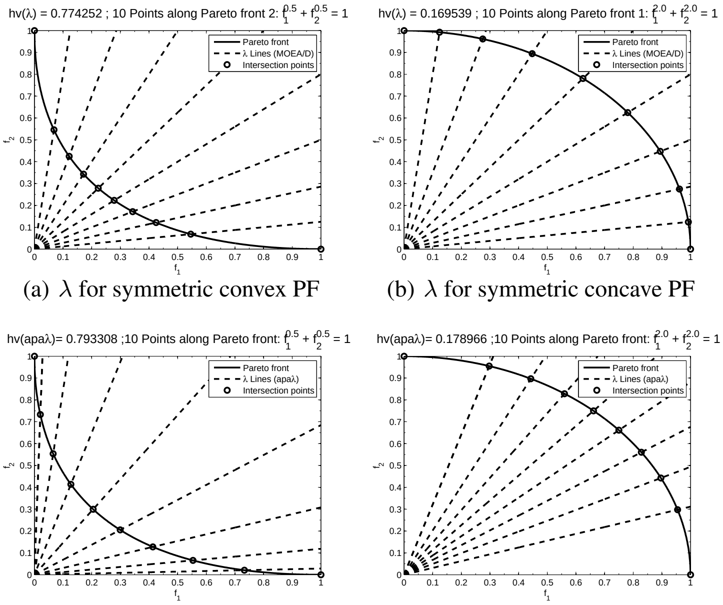

(a) λ for symmetric convex PF (b) λ for symmetric concave PF

(c) $apa\lambda$ for symmetric convex PF (d) $apa\lambda$ for symmetric concave PF

Fig. 3. 10 Points along 2-dimensional *symmetric* Pareto Fronts by λ and $apa\lambda$

In addition, further studies on MOEA/D also assert that $apa\lambda$ obtained higher hypervolume on both symmetric convex and symmetric concave PFs (Figure 3). The apa scheme is shown to significantly improve the performance of classical MOEA/D.

3.2 $apa\epsilon$-dominance: apa for ϵ-dominance

The ϵ-dominance is an advanced dominance concept that includes additive and multiplicative schemes [6]. It divides the m objective spaces into equal-sized hyper-boxes and only one solution can survive in a hyper-box. When two solutions exist in the same hyper-box and non-dominates each other, ϵ-dominance remains the one which is nearer to the corner of hyper-box. When minimizing MOPs, the additive scheme f is said to ϵ-dominate g, if $\forall i \in \{1, \cdots, m\}, f_i - \epsilon \leq g_i$.

In ϵ-dominance, the parameter ϵ is user-specific. Pareto-adaptive ϵ-dominance ($pa\epsilon$-dominance) is a new ϵ-dominance, which calculates $\epsilon^j = (\epsilon^1, \epsilon^2, \cdots, \epsilon^N)$ (N is population size) depending on the geometric characteristics of PFs [7]. When minimizing MOPs, f is said to $pa\epsilon$-dominate g in j-th hyper-box, if $\forall i \in \{1, \cdots, m\}, f_i - \epsilon^j \leq g_i$.

$pa\epsilon$-dominance handles asymmetric PFs by approximating $f_1^{p1} + f_2^{p2} = 1, p1 \neq p2$ as $f_1^p + f_2^p = 1$. Asymmetric Pareto-adaptive ϵ-dominance concept ($apa\epsilon$-dominance), on the other hand, applies the proposed apa scheme to ϵ-dominance. $\epsilon_i^j = (\epsilon_i^1, \epsilon_i^2, \cdots, \epsilon_i^N)$ in i-th objective is calculated for different shapes of PFs. When minimizing MOPs, f is said to $apa\epsilon$-dominate g in the j-th hyper-box, if $\forall i \in \{1, \cdots, m\}, f_i - \epsilon_i^j \leq g_i$.

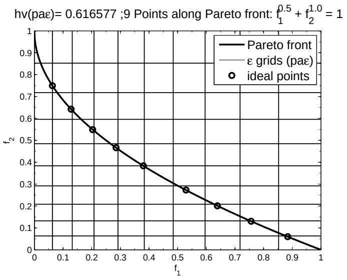

(a) $pa\epsilon$ for asymmetric convex PF

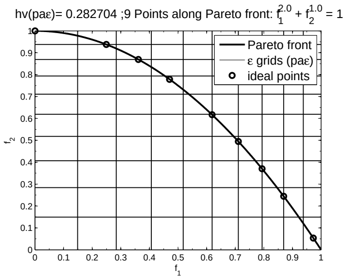

(b) $pa\epsilon$ for asymmetric concave PF

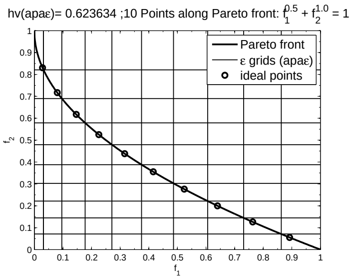

(c) $apa\epsilon$ for asymmetric convex PF

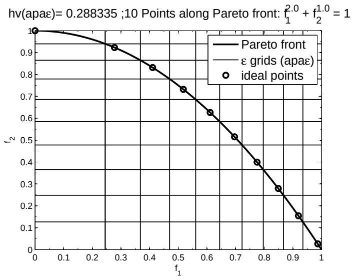

(d) $apa\epsilon$ for asymmetric concave PF

Fig. 4. Ideal Points along 2-dimensional *asymmetric* Pareto Fronts by $pa\epsilon$ and $apa\epsilon$

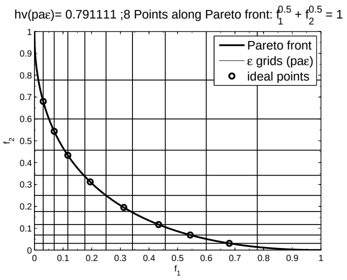

(a) $pa\epsilon$ for symmetric convex PF

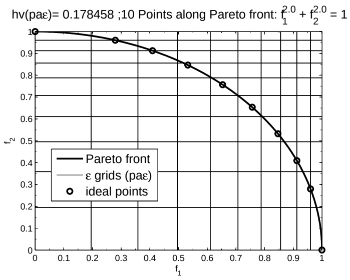

(b) $pa\epsilon$ for symmetric concave PF

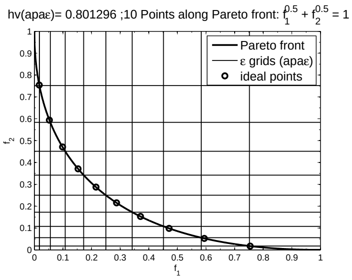

(c) $apa\epsilon$ for symmetric convex PF

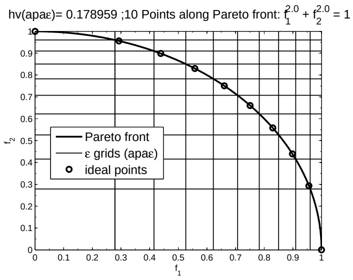

(d) $apa\epsilon$ for symmetric concave PF

Fig. 5. Ideal Points along 2-dimensional *symmetric* Pareto Fronts by $pa\epsilon$ and $apa\epsilon$

The $apa\epsilon$-dominance divides the i-th objective space into N non-equal segments (They can be equal only if $f_1 + f_2 = 1$). To begin, the apa scheme (Algorithm 1) distributes $N+1$ solutions $\{(x_i, y_i), i = 1, \cdots, N+1\}$ along the PF. Then ϵ_i^j ($i = 1, 2; j = 1, \cdots, N$) can be calculated as follows:

$$\begin{cases} \epsilon_1^j = x_{j+1} \\ \epsilon_2^j = y_{j+1} \end{cases} \quad (5)$$

Minimizing bi-objective problems, Figures 4- 5 show $pa\epsilon$ and $apa\epsilon$-dominance distribute 10 points along PFs. In some cases, $pa\epsilon$-dominance cannot get 10 points. Each ideal point is carefully drawn under ϵ-dominance concept. Only one point can survive in a hyper-box, and the point has the minimum distance to the left bottom corner of the hyper-box. For asymmetric PF, $pa\epsilon$-dominance approximates it as an symmetric PF, which has the same hypervolume as the original asymmetric PF[1]. Figures 4(a-b) show that the region near the origin $(0,0)$ is a *square*, which is obviously unsuitable for asymmetric PFs. In contrast, $apa\epsilon$-dominance arrive at *rectangle* shape (Figures 4(c-d)).

Focusing on the number of points for different PFs, $pa\epsilon$-dominance produces 9 points on the two asymmetric PFs (Figure 4(a-b)), 8 points on $f_1^{0.5} + f_2^{0.5} = 1$ and 10 points on $f_1^2 + f_2^2 = 1$ (Figure 5(a-b)), while $ap\epsilon$-dominance produces 10 points on all PFs. Comparing the hypervolume on asymmetric PFs, $pa\epsilon$-dominance obtains $hv(pa\epsilon) = 0.616577$ for $f_1^{0.5} + f_2 = 1$ and $hv(pa\epsilon) = 0.282704$ for $f_1^2 + f_2 = 1$ (Figure 4(a-b)). However, $apa\epsilon$-dominance is able to obtain higher values of $hv(apa\epsilon) = 0.623634$ and $hv(apa\epsilon) = 0.288335$, respectively (Figure 4(c-d)). In addition, for symmetric PFs, Figure 5 shows that $apa\epsilon$-dominance also obtains the higher hypervolume than $pa\epsilon$-dominance. The apa scheme is thus shown to successfully enhance the performance of Pareto dominance-based MOEAs.

4 Experimental Results and Discussion

4.1 Benchmark Problems and Experimental Setting

The experiments are performed on jMetal 3.0 [4], which is a Java-based framework that is aimed at facilitating the development of metaheuristics for solving MOPs[2]. Testing MOPs include 4 with asymmetric PFs: $f_1^{0.5} + f_2 = 1$ (ZDT1, ZDT4) and $f_1^2 + f_2 = 1$ (ZDT2, ZDT6), 4 with symmetric PFs: $f_1^{0.5} + f_2^{0.5} = 1$ (ZDT1.1, ZDT4.1[3]) and $f_1^2 + f_2^2 = 1$ (WFG4, DTLZ2.2D), and 2 discrete PFs as ZDT3 and Kursawe [4].

The classical MOEA/D - MOEA/D with the Tchebycheff approach [2] and $pa\epsilon$-MyDE [7] are included for comparison. Two instances of the apa scheme are considered here: MOEA/D with asymmetric Pareto-adaptive weight vectors ($apa\lambda$-MOEA/D) and differential evolution with asymmetric Pareto-adaptive ϵ-dominance ($apa\epsilon$-MyDE).

[1] For $f_1^{0.5} + f_2 = 1$, $pa\epsilon$ approximates it as $f_1^{0.723} + f_2^{0.723} = 1$; for $f_1^{2.0} + f_2 = 1$, $pa\epsilon$ approximates it as $f_1^{1.445} + f_2^{1.445} = 1$.

[2] http://jmetal.sourceforge.net

[3] ZDT1.1 and ZDT4.1 are symmetric PF by modifying ZDT1 and ZDT4 respectively. The true PS is formed by equally dividing circle into 200 sections in term of angle.

The experimental settings are outlined as follows. The population size is 25 and the maximum number of fitness function evaluations is $25,000$. Every algorithm runs 100 times independently for each test problem, to obtain statistically significant results. In MOEA/D, the number of neighborhoods is $T = 20$. For DE (Differential Evolution) operator, $CR = 0.25$ and $F = 0.5$. For polynomial mutation, $\eta = 20$ and $p_m = 1/n$ (n is the number of decisional variables). For apa scheme, termination condition is $\xi = 1e - 10$ and relaxing parameter to estimate PF is $\theta = 0.01$.

Five performance metrics are reported: Hypervolume (HV), Inverted Generational Distance (IGD), Generational Distance (GD), Unary Additive Epsilon Indicator ($I^1_{\epsilon+}$) and Spread. The higher Hypervolume and lower IGD, GD, $I^1_{\epsilon+}$ and Spread, the better is the algorithm's performance. The obtained results are compared using median values and the superior results of test problems are highlighted by grey background.

Table 1. Median of Hypervolume (**HV**)

	MOEA/D	$apa\lambda$-MOEA/D	$pa\epsilon$-MyDE	$apa\epsilon$-MyDE
ZDT1	$6.4496e-01$	$6.4721e-01$	$6.4576e-01$	$6.4752e-01$
ZDT4	$6.4460e-01$	$6.4690e-01$	$6.4678e-01$	$6.4828e-01$
ZDT2	$3.1346e-01$	$3.1505e-01$	$3.1417e-01$	$3.1589e-01$
ZDT6	$3.8570e-01$	$3.8558e-01$	$3.8667e-01$	$3.8713e-01$
ZDT1.1	$8.1150e-01$	$8.1937e-01$	$8.1781e-01$	$8.1880e-01$
ZDT4.1	$8.1043e-01$	$8.1879e-01$	$8.1836e-01$	$8.1896e-01$
WFG4	$2.0373e-01$	$2.0760e-01$	$2.0694e-01$	$2.0782e-01$
DTLZ2.2D	$1.9816e-01$	$2.0190e-01$	$2.0008e-01$	$2.0138e-01$
ZDT3	$5.0189e-01$	$5.0555e-01$	$4.9971e-01$	$4.9945e-01$
Kursawe	$3.8594e-01$	$3.8607e-01$	$3.8479e-01$	$3.8484e-01$

4.2 Discussions on Statistical Results

Table 1 shows the performance of the MOEAs on hypervolume. For decomposition-based algorithms, $apa\lambda$-MOEA/D reported superior HV values on 9 problems. MOEA/D fares better only on ZDT6. Both ZDT2 and ZDT6 share the same true PF of $f_1^2 + f_2 = 1$. The PF of ZDT2 exists in $f_1, f_2 \in [0.0, 1.0]$, but that of ZDT6 is in $f_1 \in [0.2809, 1.0]$ and $f_2 \in [0.0, 0.9211]$. The results indicate that Tchebycheff approach is unsuitable for dealing with disparately scaled objectives problems. To solve such problems, Zhang suggest to use the *Objective Normalization* [2].

On Pareto dominance-based algorithms, $apa\epsilon$-MyDE reported superior HV values on 9 problems, while $pa\epsilon$-MyDE fares better only on ZDT3, which has a discrete PF. The lower HV of $apa\epsilon$-MyDE on ZDT3 indicates that it is less suitable for discrete PF.

Table 2. Median of Inverted Genetic Distance (**IGD**)

	MOEA/D	$apa\lambda$-MOEA/D	$pa\epsilon$-MyDE	$apa\epsilon$-MyDE
ZDT1	$6.3658e-04$	$5.5097e-04$	$6.7638e-04$	$5.6731e-04$
ZDT4	$6.3606e-04$	$5.5161e-04$	$6.1060e-04$	$5.3733e-04$
ZDT2	$5.7958e-04$	$6.2226e-04$	$7.6548e-04$	$5.8589e-04$
ZDT6	$3.6948e-04$	$4.0058e-04$	$9.7866e-04$	$3.9867e-04$
ZDT1.1	$4.7732e-03$	$3.0518e-03$	$4.5052e-03$	$3.2133e-03$
ZDT4.1	$4.7694e-03$	$3.0493e-03$	$4.5169e-03$	$3.4396e-03$
WFG4	$4.3374e-04$	$3.8385e-04$	$4.0915e-04$	$3.9105e-04$
DTLZ2.2D	$1.4219e-03$	$1.7491e-03$	$1.7322e-03$	$1.7056e-03$
ZDT3	$2.0143e-03$	$1.5427e-03$	$2.8749e-03$	$2.7623e-03$
Kursawe	$6.5540e-04$	$6.8078e-04$	$9.7884e-04$	$8.7020e-04$

Table 3. Median of Genetic Distance (**GD**)

	MOEA/D	$apa\lambda$-MOEA/D	$pa\epsilon$-MyDE	$apa\epsilon$-MyDE
ZDT1	$1.0730e-04$	$1.3747e-04$	$9.5069e-05$	$1.0304e-04$
ZDT4	$1.8162e-04$	$1.7120e-04$	$1.0070e-04$	$9.8641e-05$
ZDT2	$9.3999e-05$	$1.0670e-04$	$9.5799e-05$	$9.2231e-05$
ZDT6	$9.6881e-04$	$8.9086e-04$	$1.0054e-03$	$1.1717e-03$
ZDT1.1	$9.5795e-03$	$8.2646e-03$	$9.3162e-03$	$8.5521e-03$
ZDT4.1	$9.4369e-03$	$8.2199e-03$	$9.1691e-03$	$8.6565e-03$
WFG4	$1.5613e-03$	$1.5306e-03$	$8.2842e-04$	$7.0187e-04$
DTLZ2.2D	$5.1184e-04$	$5.3937e-04$	$5.6100e-04$	$5.4583e-04$
ZDT3	$3.9503e-04$	$3.5437e-04$	$3.1126e-04$	$2.7977e-04$
Kursawe	$1.9408e-04$	$2.3288e-04$	$3.1429e-04$	$3.3285e-04$

Table 2 shows the performance on Inverted Genetic Distance metric. On decomposition based algorithms, $apa\lambda$-MOEA/D reported superior results on 6 problems, while MOEA/D fares better on ZDT2, ZDT6, DTLZ2.2D and Kursawe, respectively. Except the discrete PF (kursawe), these problems have concave true PFs as $f_1^2+f_2=1$ (ZDT2, ZDT6) and $f_1^2+f_2^2=1$ (DTLZ2.2D). The results indicate that the apa scheme can lead to reduce IGD performance on concave PFs.

On Pareto dominance-based MOEAs, $apa\epsilon$-MyDE got better IGD on all problems.

Tables 3 and 4 tabulated the performance of the Genetic Distance and epsilon metrics, respectively. Among the 10 test problems, $apa\lambda$-MOEA/D and $apa\epsilon$-MyDE reported superior results for these two metrics on most of the problems.

Table 4. Median of **epsilon** ($I^1_{\epsilon+}$) Metric

	MOEA/D	$apa\lambda$-MOEA/D	$pa\epsilon$-MyDE	$apa\epsilon$-MyDE
ZDT1	$3.3184e-02$	$2.0204e-02$	$3.2003e-02$	$2.6870e-02$
ZDT4	$3.3184e-02$	$2.0865e-02$	$3.1665e-02$	$2.3536e-02$
ZDT2	$2.5697e-02$	$1.9412e-02$	$3.0058e-02$	$2.0158e-02$
ZDT6	$1.9300e-02$	$2.5540e-02$	$4.3798e-02$	$1.5601e-02$
ZDT1.1	$2.9057e-02$	$5.7351e-03$	$1.2688e-02$	$7.8903e-03$
ZDT4.1	$2.9275e-02$	$6.0491e-03$	$1.1796e-02$	$1.3107e-02$
WFG4	$7.8637e-02$	$5.0718e-02$	$7.7030e-02$	$7.2197e-02$
DTLZ2.2D	$2.8321e-02$	$1.6760e-02$	$2.8834e-02$	$1.7828e-02$
ZDT3	$5.8978e-02$	$3.6942e-02$	$4.0652e-02$	$4.5659e-02$
Kursawe	$2.8456e-01$	$3.4308e-01$	$2.4865e-01$	$2.4459e-01$

Table 5 presents the performance on Spread metric, which evaluates the distribution of non-dominated solutions. On decomposition-based algorithms, $apa\lambda$-MOEA/D reported better Spread values on 6 problems, while MOEA/D on 4 namely ZDT6, WFG4, DTLZ2.2D and Kursawe. Similar to the IGD metric, the results indicate that the apa scheme may not favor Spread metric on concave PFs.

Among Pareto dominance-based algorithms, $apa\epsilon$-MyDE reported smaller Spread values on all problems. For the asymmetric problems including $f_1^{0.5}+f_2=1$ (ZDT1, ZDT4) and $f_1^2+f_2=1$ (ZDT2, ZDT6), it is worth mentioning that $apa\epsilon$-MyDE arrives at significantly better spread value than $pa\epsilon$-MyDE.

To summarize, experimental results highlight that $apa\lambda$-MOEA/D and $apa\epsilon$-MyDE are able to obtain consistently higher hypervolume, better convergence and more evenly distributed solutions than classical MOEA/D and $pa\epsilon$-MyDE on majority of the benchmark problems. The apa scheme is validated by demonstrating empirically performance improvement of both decomposition-based and Pareto dominance-based MOEAs.

Table 5. Median of **Spread** Metric

	MOEA/D	$apa\lambda$-MOEA/D	$pa\epsilon$-MyDE	$apa\epsilon$-MyDE
ZDT1	$2.8126e-01$	$8.9546e-02$	$2.4730e-01$	$1.5013e-01$
ZDT4	$2.8085e-01$	$9.0885e-02$	$2.4298e-01$	$1.3152e-01$
ZDT2	$1.3611e-01$	$1.0650e-01$	$1.9993e-01$	$9.4430e-02$
ZDT6	$1.4975e-01$	$1.6385e-01$	$1.0006e-01$	$3.8206e-02$
ZDT1.1	$6.8130e-01$	$2.9226e-01$	$4.2275e-01$	$3.3306e-01$
ZDT4.1	$6.8115e-01$	$2.9534e-01$	$4.2975e-01$	$3.6701e-01$
WFG4	$2.0255e-01$	$3.0316e-01$	$2.8014e-01$	$2.7552e-01$
DTLZ2.2D	$1.8513e-01$	$2.8223e-01$	$3.1004e-01$	$2.6857e-01$
ZDT3	$7.6543e-01$	$7.3368e-01$	$5.8611e-01$	$5.4899e-01$
Kursawe	$6.0004e-01$	$6.0182e-01$	$4.1732e-01$	$3.9657e-01$

5 Conclusion and Future Research

In this paper, we have proposed a novel Asymmetric Pareto-adaptive (apa) scheme, which automatically adjusts the position of Pareto optimal solutions according to the geometric characteristics of 2-dimensional Pareto optimal front. The new scheme is shown to work well on both symmetric and asymmetric PFs and improves the performance of general MOEAs such as decomposition-based and Pareto dominance-based MOEAs. Experimental results further confirm that the apa scheme led to significant improvements on the performance of MOEA/D and $pa\epsilon$-MyDE.

The apa scheme is showed to be efficient and for dealing with 2-dimensional MOPs. Future research is to extend the scheme to higher dimensional MOPs. Another potential further research would be to improve the MOP search based on the paradigm of Memetic Computation [8–11].

References

1. C. Coello et al. Evolutionary multi-objective optimization: a historical view of the field. IEEE Comput. Intell. Mag., 1(1):28-36, 2006.
2. H. Li and Q. Zhang. Multiobjective optimization problems with complicated Pareto sets, MOEA/D and NSGA-II. IEEE Trans. Evol. Comput., 13(2):284–302, 2009.
3. E. Zitzler and L. Thiele. Multiobjective evolutionary algorithms: A comparative case study and the strength pareto approach. IEEE Trans. Evol. Comput., 3(4):257–271, 1999.
4. J.J. Durillo, A.J. Nebro, and E. Alba. The jmetal framework for multi-objective optimization: Design and architecture. IEEE Congr. Evol. Comput., pp. 1–8, 2010.
5. J. Bader and E. Zitzler. HypE: An algorithm for fast hypervolume-based many-objective optimization. Evol. Comput., 19(1):45–76, 2011.
6. M. Laumanns, L. Thiele, K. Deb, and E. Zitzler. Combining convergence and diversity in evolutionary multiobjective optimization. Evol. Comput., 10(3):263–282, 2002.
7. A.G. HernLandez-DL.az, L.V. Santana-Quintero, C.A. Coello Coello, and J. Molina. Paretoadaptive ϵ-dominance. Evol. Comput., 15(4):493–517, 2007.
8. D. Lim, Y. Jin, Y.S. Ong, and B. Sendhoff. Generalizing surrogate-assisted evolutionary computation. IEEE Trans. Evol. Comput., 14(3):329–355, 2010.
9. Y.S. Ong, M.H. Lim, N. Zhu, and K.W.Wong. Classification of adaptive memetic algorithms: A comparative study. IEEE Trans. Syst., Man, Cybern., Part B: Cybernetics, 36(1):141–152, 2006.
10. Y.S. Ong, M.H. Lim, and XS Chen. Research frontier: memetic computation-past, present & future. IEEE Comput. Intell. Mag., 5(2):24–31, 2010.
11. G. Acampora, V. Loia, and M. Gaeta. Exploring e-learning knowledge through ontological memetic agents. IEEE Comput. Intell. Mag., 5(2):66–77, 2010.